SAND LIQUEFACTION UNDER RANDOM EARTHQUAKE LOADING CONDITION

by

K. Ishihara[I] and S. Yasuda[II]

SYNOPSIS

Several series of dynamic triaxial shear tests were run on a saturated sand using loads with irregular time history. The wave forms used were 12 records of acceleration taken at the time of Tokachioki earthquake of 1968. They could be classified as shock and vibration type wave forms and the effect of each wave form on the liquefaction potential of the sand was evaluated. In addition tests with 20 cycles and half a cycle of uniform stress application were carried out and the results were compared with those due to irregular loading.

INTRODUCTION

The shear stresses induced on a soil element in the ground during earthquakes vary erratically both in magnitude and frequency. In order to evaluate this effect on the liquefaction potential of soil deposits some averaging procedures have been employed in which a complex time history of stress change was converted into an equivalent number of constant-amplitude stress cycles (Seed-Idriss, 1971; Whitman, 1971). This equivalent load pattern has been used for testing soil specimens in the laboratory. In view of the approximate nature of this procedure, an attempt was recently made to evaluate more closely the liquefaction potential of sand subjected to loads with irregular time history (Ishihara and Yasuda, 1972). The investigation involved the use of an electro hydraulic servo-ram (or actuator) connected to the loading piston of a conventional type of triaxial cell. By employing the load variation having the same time history as the acceleration records taken at the time of the Niigata earthquake of 1964, some new features of the phenomena were made clear. Since then similar study has been in progress using several other acceleration records. This paper describes some of the new test results.

TEST EQUIPMENT AND MATERIAL

The conventional type of the triaxial shear test apparatus was incorporated into an electro-hydraulic servo loading system by which any arbitrary form of load history can be applied to the specimens in the cell. The acceleration time histories used to control the actuator load are stored on the magnetic tape. Preliminary tests showed that the loading system could not keep the applied stress perfectly controlled after the onset of liquefaction at which time the rigidity of specimens drops drastically. However, after several attempts, it was eventually found that the use of an elastic rubber joint in the loading ram could correct the difficulty. All the test results described herein are those obtained by using this improved system. The actuator is capable of producing 300 kg of dynamic force and 410 kg of static

[I] Associate Professor of Civil Engineering, University of Tokyo, Bunkyo-ku, Tokyo.

[II] Graduate Student of Civil Engineering, University of Tokyo, Bunkyo-ku, Tokyo.

force. The travel of the piston is ±1.5 cm. The triaxial test specimens, 5 cm in diameter by 10 cm long, were prepared by pouring the boiled saturated sand into a forming mold filled with de-aired water. The specimen with a given density was consolidated under a confining pressure of 1.5 kg/cm^2, and then subjected in undrained condition to an axial load with specified time history and varying at the same rate as actually recorded. In each test the axial stress, axial strain, and pore pressure were measured by appropriate transducers and recorded by an oscillograph. The sand (Fuji river sand) used consists of subangular particles with the specific gravity of 2.73. The maximum and minimum void ratios are 1.03 and 0.48, respectively. The particle size distribution is shown in Fig.1. The void ratios of the test samples are 0.78 to 0.81 corresponding to the relative densities of 40 to 45 %.

EARTHQUAKE RECORDS USED IN TESTS

The Port and Harbor Research Institute had installed strong motion accelerograms at several ports in the northern part of Japan and secured several acceleration records at the time of the Tokachioki earthquake of 1968. The load patterns used for the present dynamic tests are those which were obtained on the sandy ground at the sites shown in Fig.2, where the ground water tables were all high. At the time of the earthquake, no liquefaction was observed directly, but there were several features of damage which seem to indicate that liquefaction must have occurred at least partly. Three seismographic stations felt the main shock at 9:49 a.m. on May 16, 1968 and monitored the accelerations of 209 to 213 gal in the N-S direction and 140 to 188 gal in the E-W direction. These records were all used for the present investigation and their wave forms are shown in Figs.4 to 6. The instant of time at which the maximum acceleration occurred is indicated by an arrow and the time scale shown is based on the elapse of time from the start of recording. Among many aftershocks, the one which hit the area at 7:39 p.m. on the same day was the second greatest, and its records at Aomori and Muroran were also utilized for the present study as well as a record from Hachinoe which was taken at 10:42 p.m. on June 12, 1968. The actual records of these earthquakes, whose maximum accelerations are from 35 to 95 gal, are shown in Fig.3. In addition to the tests using these records, similar tests were run by employing sinusoidally changing cyclic stress with constant amplitude.

TEST PERFORMANCE

In the complicated time history of an earthquake record, it is always possible to locate the biggest spike where the maximum acceleration occurs. When this record is to be converted to the up-and-down movement of the triaxial loading piston, there are two ways of doing this: one is such that the maximum deviator stress corresponding to the maximum acceleration is attained when the piston reaches the lowest position; and the other is such that the direction of the maximum acceleration is oriented so as to coincide with the highest position of the loading piston. The former type of test will be referred to as CM-tests and the latter as EM-tests. It is worthy of notice that these two types of loading developed different pore pressure although the load pattern employed was the same. Hence, it was considered necessary to perform tests separately for each of these cases. The tests were carried out by first setting the axial load intensity at an appropriate level which would not induce liquefaction through the entire duration of loading. The changes in pore pressure, u, with time obtained in some of these tests using the acceleration records from Aomori are shown in Fig. 4(b), (d), (g), and (i). In these figures, the maximum stress ratios, $\sigma_{max}/2\sigma_c$, used in the tests are indicated. σ_{max} is the maximum dynamic deviator stress and σ_c denotes the confining pressure. Also, the maximum pore pressure developed during each test was observed and is plotted in Fig.7 against the maximum stress ratio. During the next series of tests the level of load intensity was raised a little and the load, having the same wave pattern as before, but with a greater amplitude, was applied to new samples prepared under nearly identical conditions. Again, the maximum stress ratio and the pore pressure finally developed were observed and are plotted in Fig.7. After repeating this procedure several times, each time with increased load level, liquefaction could be brought about. At this time the induced pore pressure became equal to the confining pressure. Recorded results of tests in which liquefaction occurred are shown in Fig. 4(c), (e), (h), and (j) for the wave forms obtained at Aomori. Similar test results using the acceleration records of the main shock at Muroran and Hachinoe are shown in Figs. 5 and 6. Additional series of tests were made using the acceleration records obtained in the aftershock of the Tokachioki earthquake of 1968, whose wave forms are shown in Fig.3. The results are summarized in Fig. 7.

TEST RESULTS AND DISCUSSIONS

A typical test result is presented in Fig.6(e) which shows that the pore pressure builds up abruptly at the instant when the peak acceleration occurs without any pore pressure previously developed. This can be accounted for by the fact that the maximum acceleration occurs suddenly like an impulse, see Fig.6 (a). This type of loading will be referred to as a shock type loading. When the input stress varies more uniformly as shown in Fig.5(f) the pore pressure increases gradually with time as shown in Fig.5(j). This type of change in stress will be called a vibration type loading. All of the wave patterns used in the study were classified into one of these two groups in accordance with the following rule: Consider only the part of the time history which has the same sign as the maximum stress (acceleration). If, preceding the maximum acceleration, there exist only one or two peaks whose amplitude is greater than 60 % of the maximum, the wave is defined as being of the shock type. Conversely, if more than three peaks having the amplitude greater than 60 % of the maximum are included in the wave form on the side of the maximum acceleration, the wave is referred to as being of the vibration type. The classification of each wave form is given in Table 2, which shows that most of the wave forms recorded during the main shock belong to the shock type, while those due to the aftershocks are of the vibration type. Figures 7(a) to (d) summarizes all the test results. The data is arranged according to the above classification. The figures show that the pore pressure which ever develops after the load has been applied increases as the applied stress ratio, $\sigma_{max}/2\sigma_c$, is raised stepwise. The stress ratios denoted by σ_{max}, $l/2\sigma_c$, at which liquefaction eventually sets in were determined for each wave form by extrapolating the data curves shown in Fig.7, and these values are listed in Table 2. The average value of the stress ratio at liquefaction corresponding to each type of test (CM or EM-test) and wave form (shock or vibration) is indicated in each of Figs.

7(a) to (d). The data yield the important information that the shock type wave form requires a greater stress ratio for liquefaction than the vibration type wave form both in the CM and EM-tests. The average stress ratios at liquefaction are 0.31 and 0.27 respectively, for the shock and vibration types of the wave form.

In order to investigate this point further additional tests were run in which the stress ratios required to cause liquefaction under 20 cycles and a single half cycle of sinusoidal loading were determined. Because of the asymmetrical nature of the response of triaxial samples, the stress ratio due to half a cycle was greater on the compression side than that on the extension side. Since the stress ratio in the former condition is to be compared with the stress ratio in CM-tests, the test result is indicated in Figs.7(a) and (c) together with the result of CM-tests. For the same reason, the stress ratio due to half a cycle on the extension side is shown in Figs.7(b) and (d) together with the result of EM-tests. The observed stress ratio corresponding to liquefaction after 20 cycles did not differ significantly whether the first pulse is directed towards the compression or extension side. Therefore, the result of this type test is indicated all in Fig.7. Fig.7 shows that the stress ratio due to half a cycle and 20 cycles limits, respectively, the upper and lower bounds of all the stress ratios which can be attained in any type of random loading. When several pulses occurred before the maximum stress, their effect on the pore pressure development was found to be more pronounced if their amplitude was large. The tests with uniform stress application can be considered to be the case in which the effect of previous pulses is the greatest. In contrast, the tests with half a cycle of loading, involving no previous pulses, can be considered to be the tests without any effect of previous stress history. In view of this, the above test results provide good evidence that the stress ratio at liquefaction under any random loading lies between the two extremes defined above, and that the test with the vibration type load tends to give smaller stress ratio at liquefaction than the tests with the shock type load.

Figs.7(a) to (d) also show that the difference in the stress ratio between the CM and EM-tests is more pronounced in the case of the shock type than in the vibration type of loading. This tendency is consistent with the fact that the greatest difference in the stress ratio between the CM and EM-tests occurs in the test employing half a cycle and there is no such difference in the test with 20 repetition of uniform stress application. It is of interest to compare the stress ratio in each case with that corresponding to 20 repetitions of uniform stress application. The ratios between these two stress ratios are shown in Table 2. They were obtained by taking averages between CM and EM test results. The overall averages for the data obtained in this study are 0.53 and 0.61 for the shock and vibration type of loading, respectively.

CONCLUSIONS

Dynamic triaxial shear tests have been performed on a saturated sand using loadings with various kinds of irregular time history resembling the histories which actually occur during an earthquake. The maximum stress required to cause liquefaction was compared with the similar amplitude determined from tests in which the sand was subjected to 20 cycles of uniform amplitude loading. It was found, that for the case of shock loading, defined as a loading in which the maximum stress builds up in a few cycles, the corresponding 20-cycle failure amplitude ranged between 47 and 61 % of the maximum stress of the irregular load. The corresponding ratio for the case when the stress builds up more slowly is in the range of 56 to 65 %. These ratios may be useful for estimating the liquefaction potential of sand during earthquakes using test data from the more conventional constant amplitude tests.

ACKNOWLEDGEMENTS

The work described in this paper was partly sponsored by the research grant from the Ministry of Education. The acceleration records used in this study were provided by Dr. H. Tsuchida of the Port and Harbor Research Institute. The original draft of this paper was critically reviewed and edited by Professor John Lysmer of University of California. The writers are most grateful to them and for the assistance of Mr. Takao Kubo in carrying out the experiments.

REFERENCES

1. Seed, H. B. and Idriss, I. M., Simplified Procedure for Evaluating Soil Liquefaction Potential, Proc. of ASCE, SM9, 1971, pp.1249-1273.
2. Whitman, R. V., Resistance of Soil to Liquefaction and Settlement, Soils and Foundations, Vol. 11, No. 4, 1971, pp.59-68.
3. Ishihara, K. and Yasuda, S., Sand Liquefaction Due to Irregular Excitation, Soils and Foundations, Vol. 12, No. 4, 1972, pp.65-78.
4. Tsuchida, H., Kurata, E. and Sudo, K., Strong-Motion Earthquake Records on the 1968 Tokachi-oki Earthquake and its Aftershocks, Technical Note of The Port and Harbour Research Institute, No. 80, June, 1969.

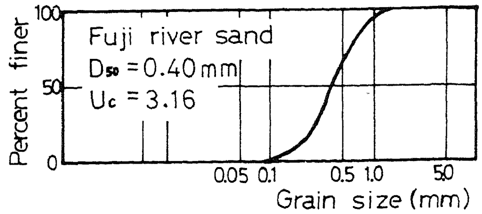

Fig.1 Grain size distribution

Table 1 Wave form used in the test

Site			Date and time	a_{max} (gal) NS	a_{max} (gal) EW
Aomori	S235	M.S.	5.16, 9:49	213	180
〃	S264	A.S.	〃 19:39	56	86
Muroran	S234	M.S.	〃 9:49	209	140
〃	S241	A.S.	〃 19:39	95	62
Hachinohe	S252	M.S.	〃 9:49	235	188
〃	S310	A.S.	6.12, 22:42	35	30

M.S.: Main shock , A.S.: After shock

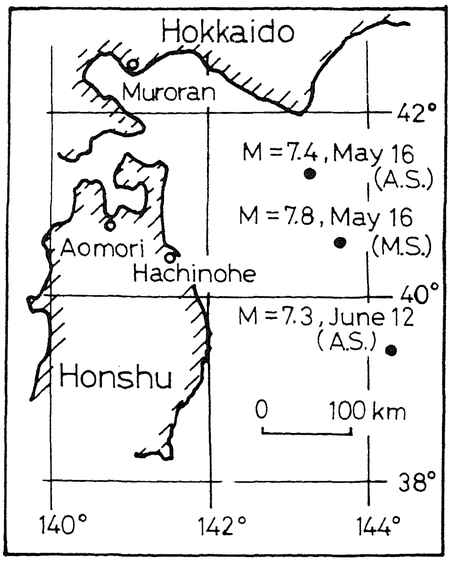

Fig.2 Location of epicenters and accelerometers

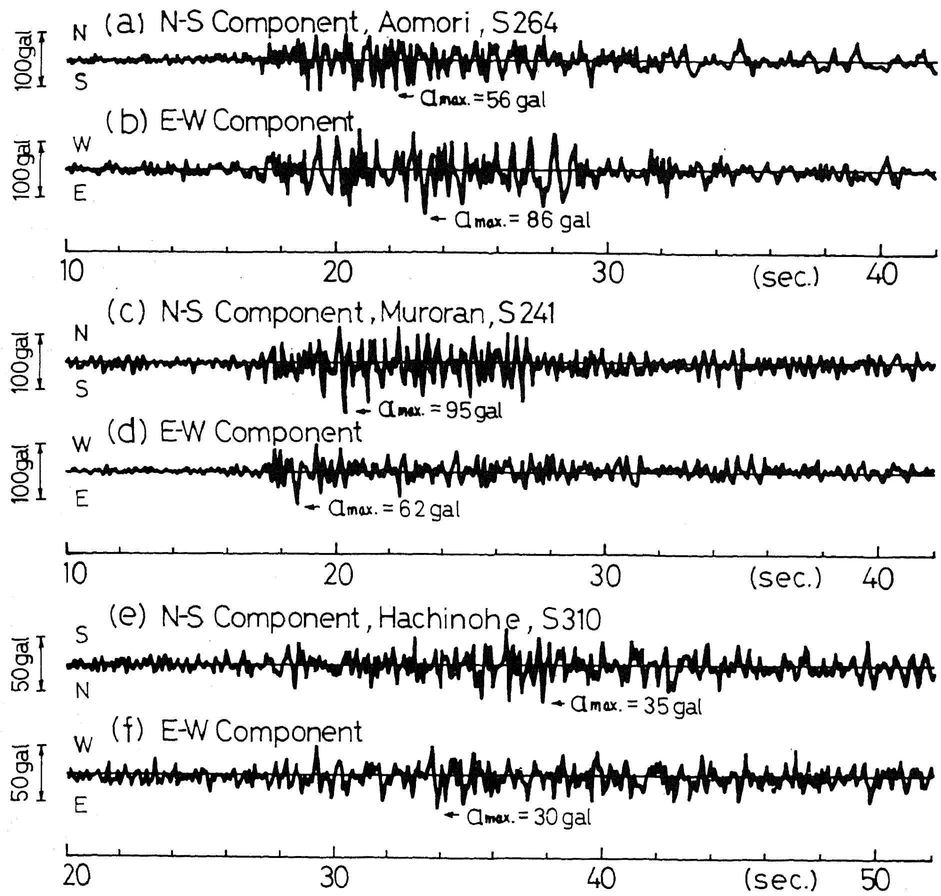

Fig.3 Acceleration records (Aftershocks, Tokachioki earthquake of 1968)

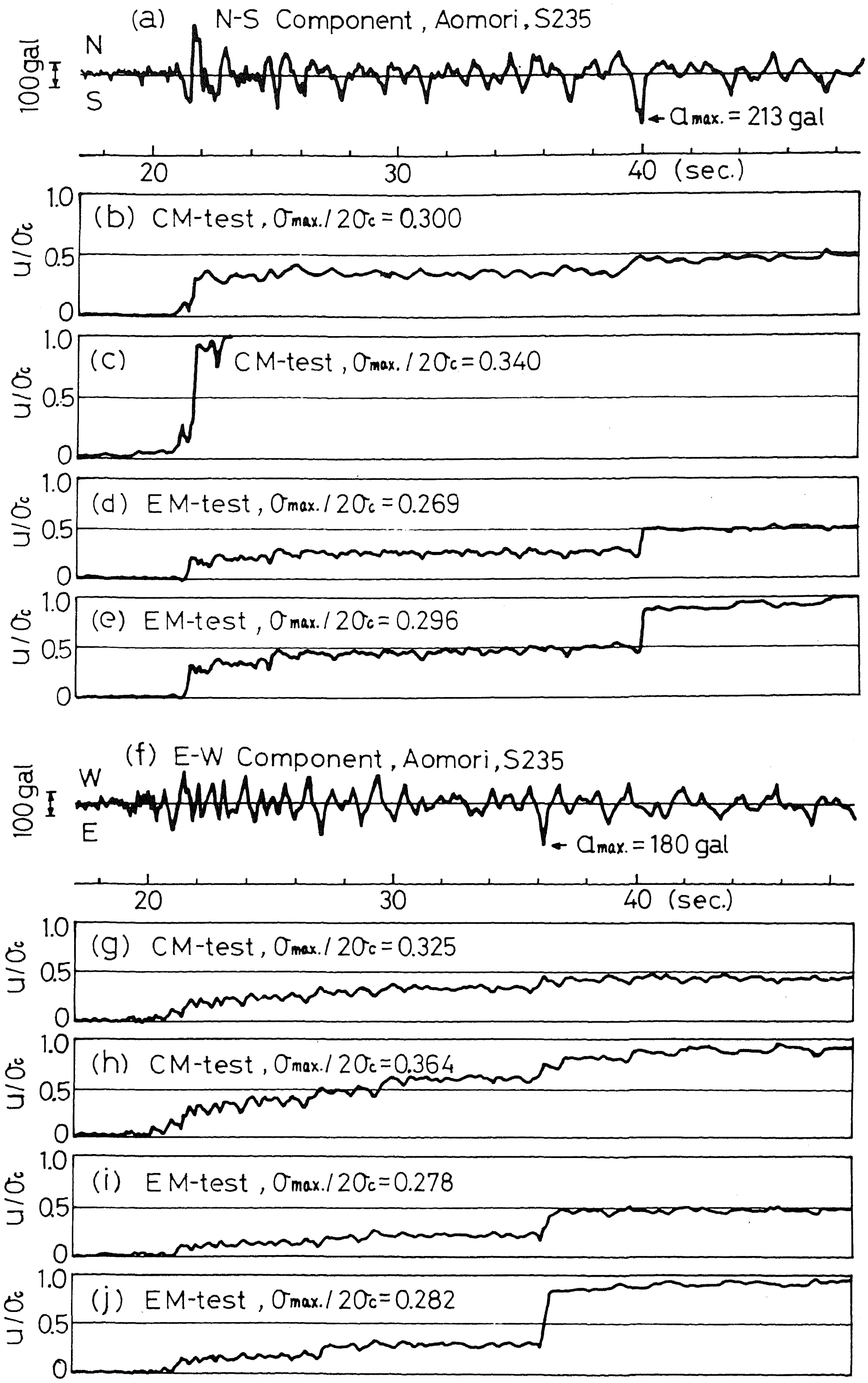

Fig.4 Recorded accelerations and pore pressure (Main shock, Tokachioki earthquake, 1968, Aomori S235)

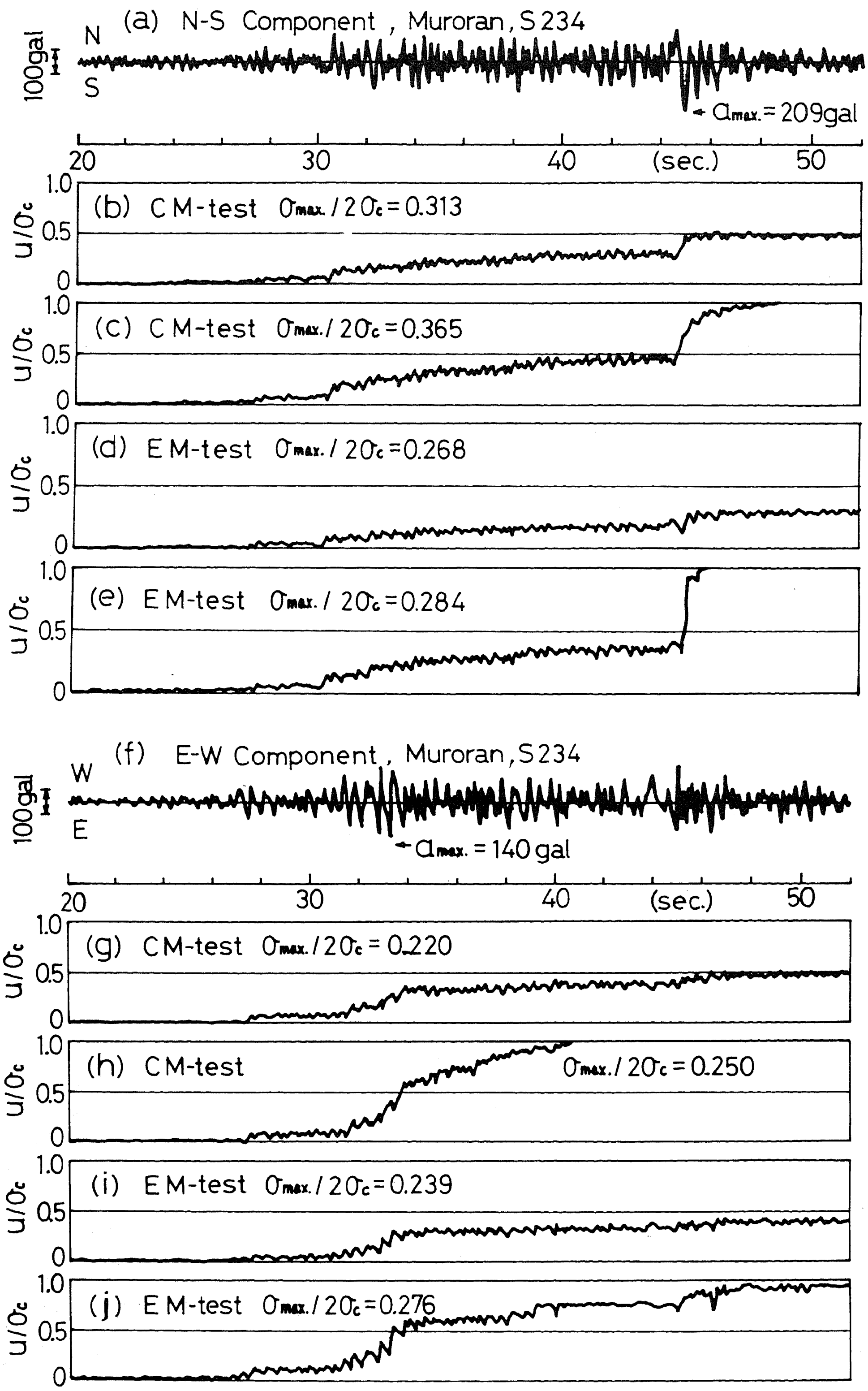

Fig.5 Recorded accelerations and pore pressure (Main shock, Tokachioki earthquake, 1968, Muroran S234)

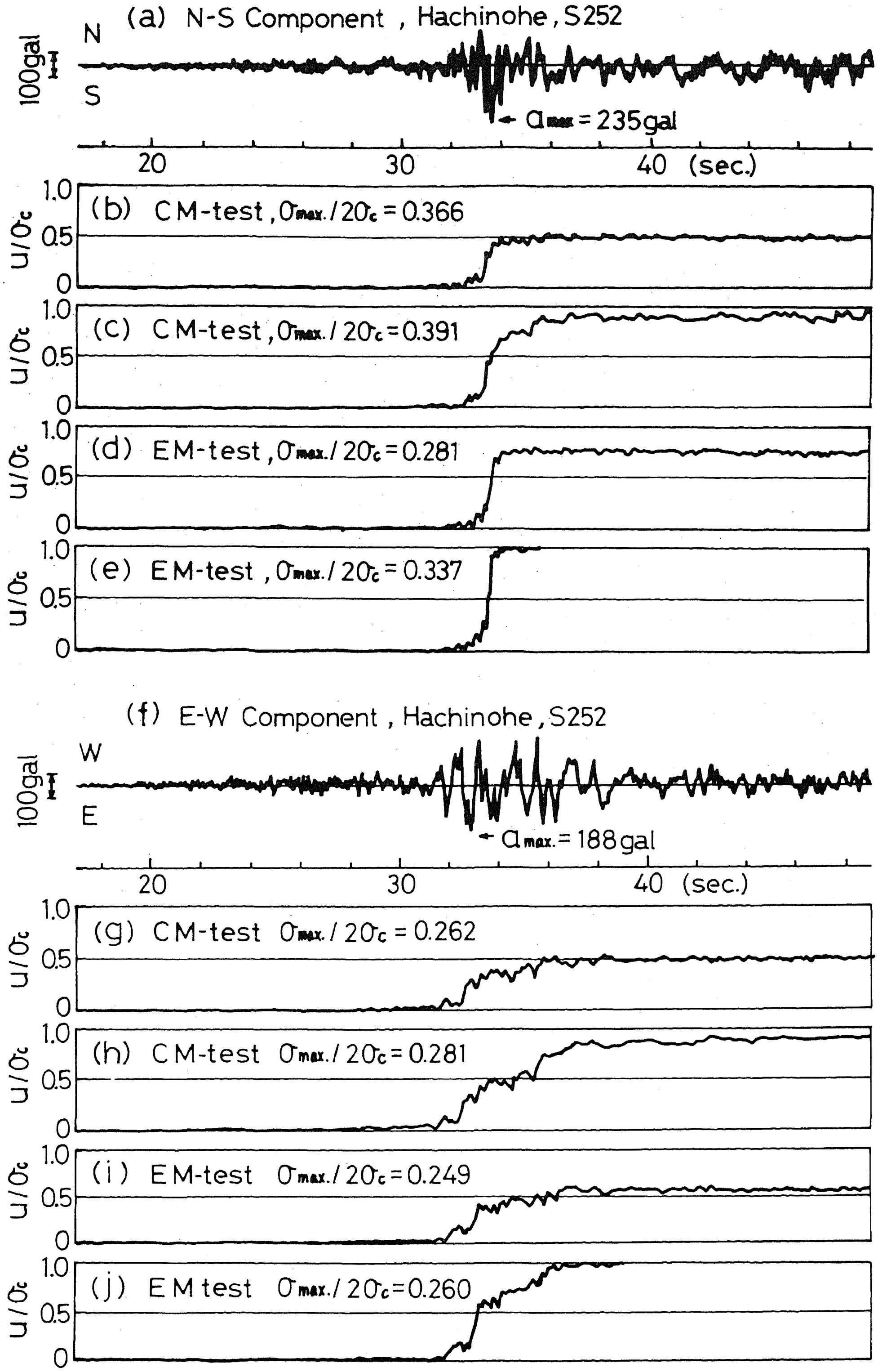

Fig.6 Recorded accelerations and pore pressure (Main shock, Tokachioki earthquake, 1968, Hachinohe S252)

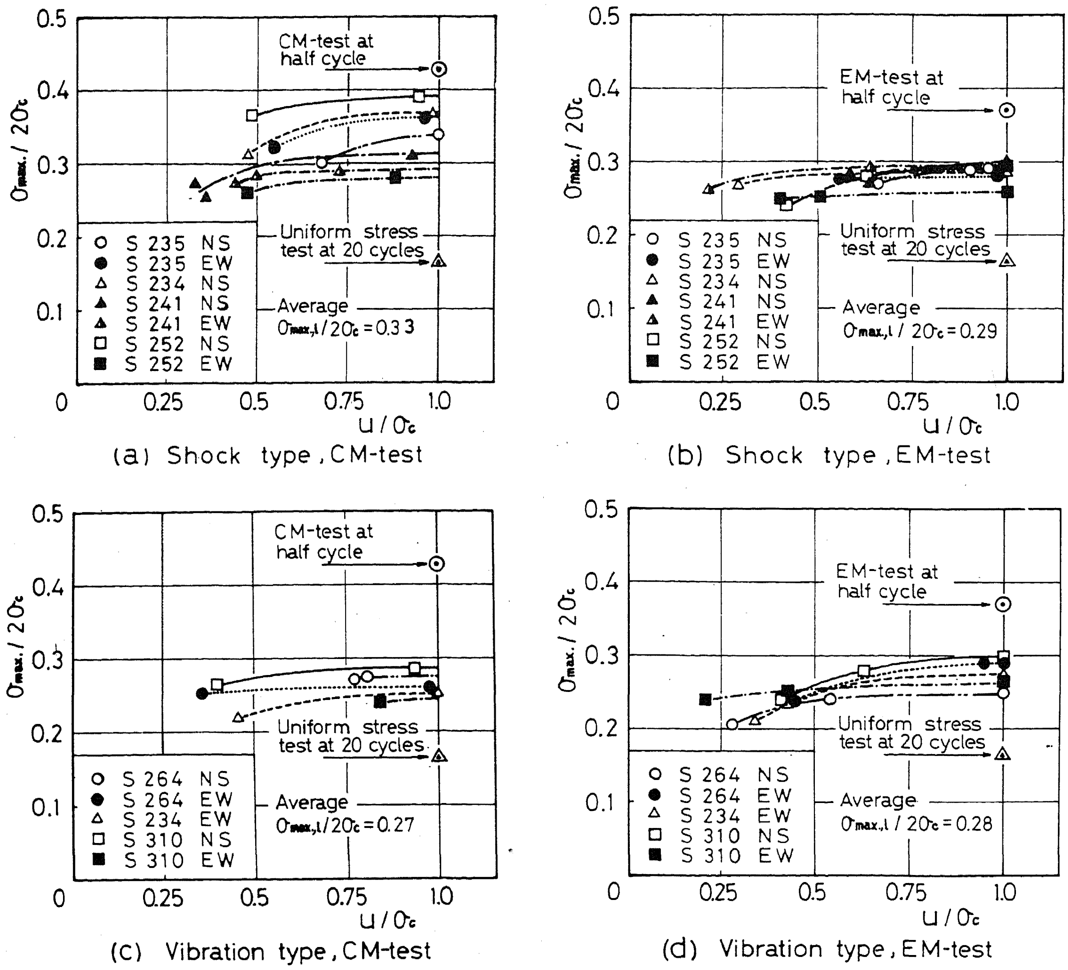

Fig.7 Relations between stress ratios and pore pressures

Table 2 Summary of test results

Site	Symbol	N-S Component				E-W Component			
			CM	EM	$\sigma_{dp,l}/\sigma_{max,l}$		CM	EM	$\sigma_{dp,l}/\sigma_{max,l}$
Aomori	S235	S*	0.34	0.30	0.52	S	0.36	0.28	0.52
	S264	V**	0.28	0.25	0.62	V	0.26	0.29	0.60
Muroran	S234	S	0.37	0.28	0.51	V	0.25	0.28	0.63
	S241	S	0.31	0.30	0.54	S	0.29	0.29	0.57
Hachinohe	S252	S	0.39	0.31	0.47	S	0.28	0.26	0.61
	S310	V	0.29	0.30	0.56	V	0.25	0.26	0.65

* Shock type load ** Vibration type load

$\sigma_{dp,l}/2\sigma_c = 0.165$, (20 cycles of uniform stress, $\sigma_{dp,l}$)